

Dynamic scaling theory of the Kosterlitz-Thouless-Berezinskii transition: ubiquitous finite size effects

Louis Colonna-Romano,^{*} Stephen W. Pierson,[†]

Department of Physics, Worcester Polytechnic Institute, Worcester, MA 01609-2280

Mark Friesen[‡]

University of Wisconsin, Madison, WI 53706

(Received March 21, 2022)

A numerical study of the neutral two-dimensional (2D) lattice Coulomb gas is performed to examine dynamic scaling, finite size effects, and the dynamic critical exponent z of the Kosterlitz-Thouless-Berezinskii transition. By studying large system sizes ($L = 100$), we show $z = 2.0 \pm 0.2$ using Fisher-Fisher-Huse (FFH) scaling. We also present evidence that the vortex correlation length is finite below the transition temperature, in contrast to conventional wisdom. Finally, we conclude that previous findings for a variety of experimental systems that $z \simeq 5.6$ using FFH scaling indicates that finite size effects are ubiquitous in 2D superconductors and Josephson Junction Arrays.

I. INTRODUCTION

The universality class of the two-dimensional (2D) XY model has been fascinating from the start with its phase transition being driven by topological excitations, the unusual, exponential temperature dependence of the correlation length, and its apparent presence in systems ranging from 2D superfluids and superconductors to liquid crystals and magnetic systems.^{1–3} Despite its uniqueness, the detection of the Kosterlitz-Thouless-Berezinskii (KTB) transition,^{1–3} characterized by an unbinding of vortex pairs, has been challenging, but several techniques have been developed to probe its critical behavior. In two-dimensional superconductors and Josephson Junction arrays (JJA's), an examination of the dc transport properties in zero magnetic-field has been the primary method, but the magneto-resistance⁴ and the ac kinetic inductance⁵ have also been used. More recently, magnetic flux noise measurements⁶ have been used to study the KTB transition. And, as we discuss shortly, numerical methods and scaling approaches have also been used. The advantage of the scaling methods is that they can reveal information on the dynamic critical exponent z , one of the key exponents in the KTB critical behavior, which relates the relaxation time τ to the vortex correlation length ξ via $\tau \propto \xi^z$.

While there are many methods for studying the KTB transition,⁷ the most common is the “conventional” method which involves an analysis of the dc voltage-current (V - I) isotherms and the temperature dependent resistance $R(T)$. In this approach, the transition temperature T_c is determined via the V - I exponent $\alpha(T, I)$ ($V \propto I^\alpha$), which is predicted to have a value of 3 at T_c (assuming $z = 2$), and whose value should decrease rapidly for weak currents near T_c . The Ohmic resistance is then fitted by the Kosterlitz² or Minnhagen form⁷ for the resistance, which are respectively, $R \propto \exp[-bz/\sqrt{T - T_c}]$ and $R \propto \exp[-bz\sqrt{(T_{c0} - T_c)/(T - T_c)}]$, where b is a

system-specific parameter and T_{c0} is the mean-field transition temperature.

There are many weaknesses to the conventional approach.⁸ For example, it is valid only in the weak-current limit where few experiments can probe effectively and where finite-size effects dominate. Moreover, the exponent α has a current dependence and so determining its value uniquely for a given temperature is not possible. In fact, researchers can use this flexibility to their advantage to show a rapid variation of α with temperature near T_c . This is done by determining α in different current ranges for each temperature so as to achieve the desired behavior. (The most accurate method would be to determine α for the V - I isotherms for the same current so as to represent a single length scale.⁸) Another problem with the traditional approach is the number of fitting parameters in the resistance formulas, which allow excessive freedom for interpreting results. For these reasons, it is important to examine other approaches to verifying and studying KTB behavior.

The Fisher-Fisher-Huse (FFH) dynamic scaling,⁹ which says that $V\xi^z/I$ is a function of $I\xi/T$, has its advantages over the conventional approach. The most prominent is that it is valid over an extended current range and therefore incorporates the current dependences of $\alpha(T, I)$. Moreover, FFH scaling can be used to determine z . Recently, it has been used to study experimental, dc V - I data but yields a large value of the dynamic critical exponent $z \simeq 5.6$ for a wide variety of samples and systems.^{8,10,11} It has recently been reiterated that the FFH scaling is only valid in the absence of finite size effects and suggested that finite size could result in large values of z .¹²

Finite size effects, which include a finite size system and the inherent magnetic penetration depth λ_\perp ¹³ in superconductors, have long been known to complicate the verification of KTB behavior because they make free vortices possible for any temperature range. Kadin *et al.*¹⁴ and Lee and Garland⁴ were among the first to study

this experimentally while Repaci *et al.*¹⁵ and Herbert *et al.*¹⁶ have recently extended this work. Theoretically, Simkin and Kosterlitz¹⁷ have investigated numerically and analytically the finite size effects in these systems, while Artemov¹⁸ has examined the effect of “Pearl” vortices on the magnetization in superconducting thin films. And more recently, Pierson and Valls¹⁹ have completed a renormalization group study of the two-dimensional Yukawa Gas, which incorporates the inherent finite size λ_{\perp} into the two-dimensional Coulomb Gas (2DGG).

Finite size (FS) scaling, which incorporates the effect of a finite size into the FFH scaling, is an established method in the study of numerical data in KTB behavior. Lee and Teitel²⁰ were among the first to use this approach to show that the dynamic critical exponent z has a value 2 for the two-dimensional Lattice Coulomb Gas (2DLCG). Medvedyeva *et al.*¹² have also used finite size scaling to reinforce the result $z = 2$ for the 2D resistively-shunted-junction model. (Numerical studies in fact have provided many insights into KTB behavior. A review of those results is beyond the scope of this paper but we refer the reader to many excellent papers in the literature.^{21–26})

Like the conventional approach and FFH scaling, FS scaling has its strengths and weaknesses. For example, because FS scaling requires the ability to carefully tune the system size, it is not conducive to studying experimental data where the finite length scales are more illusive. It is therefore important to keep in mind that all approaches provide a great deal of information and often complement one another.

The correlation length is an important quantity in FFH scaling but questions about its form below T_c remain. In the original paper of Kosterlitz,² the correlation length was taken to be infinite below the transition temperature owing to the divergence of the susceptibility there. In subsequent papers by Friesen,²⁷ Pierson,²⁸ and Simkin and Kosterlitz,¹⁷ the vortex correlation length is taken to be finite for this temperature regime (but still diverging at T_c from below) and interpreted roughly as the size of the largest vortex pairs. Other authors¹² maintain that the correlation length is infinite for $T < T_c$.

In this paper, we do a numerical study of the 2DLCG using Monte Carlo simulations to understand the difference in the value of z obtained from finite size scaling and FFH scaling. We vary the system size to study the effect of finite sizes and verify that $z = 2$ using FFH scaling, thereby making FFH scaling consistent with FS scaling. We also analyze the transport characteristics and find evidence that the vortex correlation length is finite below the phase transition, in contrast to the claims of others.¹² The numerical approach that we use is that of Lee and Teitel^{20,22} extended to larger system sizes ($L = 200$).

The paper is organized as follows: Section II describes the model that we use along with the numerical and scaling methods. In Section III, we present our results and analysis of the transport characteristics. Implications and a summary of our work is presented in Section IV.

II. MODEL AND METHODS

A. 2D Lattice Coulomb Gas with an applied field

To study the KTB critical behavior and its dynamic critical exponent, we use the 2DLCG model, whose relationship to the KTB transition and mapping to the 2DXY model are well known.^{20,29} This model is described in Refs. 20 and 22 and so will be only briefly described here.

The Hamiltonian for the 2DLCG is given by

$$H = \frac{1}{2} \sum_{i,j} q_i V(\mathbf{r}_{ij}) q_j, \quad (1)$$

where the sum is over all pairs of sites in the lattice, q_i is the (integer) charge at site i , $\mathbf{r}_{ij} = \mathbf{r}_i - \mathbf{r}_j$, and \mathbf{r}_i is the location of the i th charge. V , which solves the discrete form of Poisson’s equation in two dimensions, is the Coulomb potential (and is therefore logarithmic at large distances). Using Fourier transforms, V in Eq. (1) may be replaced by

$$V(\mathbf{r}) = \frac{1}{N} \sum_{\mathbf{k}} V_{\mathbf{k}} (e^{i\mathbf{k} \cdot \mathbf{r}} - 1) \quad (2)$$

where, for the square lattice considered here,

$$V_{\mathbf{k}} = \frac{\pi}{2 - \cos(\mathbf{k} \cdot \hat{\mathbf{x}}) - \cos(\mathbf{k} \cdot \hat{\mathbf{y}})}. \quad (3)$$

The wave vectors are defined in the usual way:

$$\mathbf{k} = \frac{2\pi m_1}{L} \hat{\mathbf{x}} + \frac{2\pi m_2}{L} \hat{\mathbf{y}}, \quad (4)$$

where $m_1, m_2 = 0, 1, 2, \dots, L - 1$. In addition, since we wish to apply our results to 2D superconductors in zero-magnetic field, we use the constraint that the total charge in the system must be zero, which deals with the infrared divergence as $\mathbf{k} \rightarrow 0$.

In the presence of an electric field, \mathbf{E} , an electric potential energy term of the form $\sum_i q_i \mathbf{r}_i \cdot \mathbf{E}$ is added to the Hamiltonian.²⁰ The new term results in a net movement of charge along the direction of the field \mathbf{E} that we measure in terms the charge current density, \mathbf{J} , using the approach of Ref. 20.

The applied field E and the resulting vortex current density J in the 2DLCG model are analogous to the current I and voltage V in a superconducting thin film, but in an inverted way due to the mapping between the two systems. In the superconducting thin film, the current is injected into the sample, which causes vortex movement in a direction perpendicular to the current via the magnus force. This results in resistance and therefore a voltage V . For the 2DLCG, it is the voltage that is applied and that results in the vortex “charge” current in a direction parallel to the electric field. Following the notation of Lee and Teitel,²⁰ the following correspondences

between the two systems apply: $E \longleftrightarrow I$ and $J \longleftrightarrow V$. In this paper, we will examine the E - J curves of the 2DLCG, which correspond to V - I characteristics in actual superconducting thin films. Unless otherwise noted, the notation that we use will be that of the 2DLCG. Along these lines, the E - J curves will be plotted as E versus J in our figures, so that they mirror the analogous curves in the 2D superconductors that are plotted as V versus I . We will therefore use the notation V - I for the current-voltage curves instead of the more standard I - V .

B. Monte Carlo Simulations

The Metropolis³⁰ Monte Carlo technique is used to calculate the J - E data based on the Hamiltonian discussion in Section IIA. Briefly, the technique, as it applies to the 2DLCG model with a square ($N = L \times L$) lattice and integer charges, is as follows: (See Ref. 20 for more details.)

1. Create a trial system from the original system by choosing a site, i , and one of its four neighbors, j , at random. Add one unit of charge to site i and subtract one unit from site j so that the net charge in the system is always zero.
2. Compute $\Delta H = H_{\text{trial}} - H_{\text{original}}$. Since only two sites have been altered, most terms in H_{trial} and H_{original} are the same, simplifying the calculation of ΔH .
3. If $\Delta H < 0$ or if $e^{-\Delta H/T}$ is greater than a random number uniformly distributed on the interval $[0, 1]$, accept the change and replace the the original system with the trial system for subsequent trials. Otherwise, leave the system unchanged.

When evaluating the Hamiltonian for a trial system, the minimum image convention and toroidal (periodic) boundary conditions are used.³¹ In addition, a “stability” term of the form $\sum_i (q_i^4 - q_i^2)$ is added to the Hamiltonian to minimize the probability of creating multiply charged sites in the system.²²

For many combinations of E and T , particularly when the charge density is small, a low rate of acceptance of trials is expected. When this occurs, it is convenient to calculate ΔH without summing over the array. The method employed here, used and described by Lee and Teitel,²² is to store information on each site in the system in the form of the potential, which is updated for each site after each accepted trial. This technique can improve run times on the order of the reciprocal of the acceptance ratio, often factors of $O(10^3)$ or more.

A sequence of N trials is called one Monte Carlo Step (MCS). All of our computer runs consist of an initial 10,000 MCS to equilibrate the system during which no data are saved, followed by at least 500,000 MCS, for which the average current is computed. The only exceptions were some large systems ($L = 200$) at $E > 0.6$

where a smaller number of MCS was used due to very long run times. At high electric field, the current is large and the shorter runs provide sufficient accuracy. At each E and T , at least five runs were performed. The error bars on the points in Figure 1, Figure 4, and Figure 5 are the standard deviations of the average current from these runs. In some cases at low E , many additional runs were performed in an attempt to reduce the error bars.

C. Fisher-Fisher-Huse and Finite-Size Scaling Methods

Given the difficulties of the conventional approach to analyzing V - I characteristics discussed in Section I, it is important to use other methods including the powerful scaling methods. In this paper, we will use Fisher-Fisher-Huse scaling and finite size scaling.

In the FFH theory,⁹ for 2D superconductors, the E - J (in the notation of the 2DLCG) curves should scale as

$$J = E\xi^{-z}\chi_{\pm}(E\xi/T), \quad (5)$$

where $\chi_{+(-)}(x)$ is the scaling function for temperatures above (below) T_{KTB} . The two important asymptotic behaviors of $\chi(x)$ are $\lim_{x \rightarrow 0} \chi_{+}(x) = \text{const.}$ (Ohmic limit), and $\lim_{x \rightarrow \infty} \chi_{\pm}(x) \propto x^z$ (critical isotherm). As established in previous papers,^{8,10,11} it is advantageous to rewrite Eq. (5) as

$$\frac{E}{T} \left(\frac{E}{J} \right)^{1/z} = \varepsilon_{\pm}(E\xi/T) \quad (6)$$

(where $\varepsilon_{\pm}(x) \equiv x/\chi_{\pm}^{1/z}(x)$) because only the x -scale is stretched in Eq. (6). In Eq. (5), both the x -scale and y -scale are stretched making it harder to judge a collapse of the scaled data.

The FFH scaling has three fitting parameters z , T_c , and b , which can be determined in the three scaling steps. The first, which yields estimates of z and T_c , is to determine the critical isotherm. In the absence of finite size effects, the critical isotherm is straight on a log-log plot since $J \propto E^{z+1}$ for all E at $T = T_c$. The second step is to estimate b in the exponent of the correlation length, which, for experimental data, one can do by examining the resistance since $R(T) \propto \xi^{-z}$. For numerical data, one assumes $\xi \propto \exp[C/|T - T_c|^{1/2}]$,^{11,20} which is generally expected to hold for $T > T_c$. The final step is to achieve a scaling collapse for Eq. (6), adjusting the three parameters within the error bars established in steps 1 and 2. One should also bear in mind that all these steps can be repeated to optimize the scaling collapse.

In the finite size scaling form, valid for $\xi > L$, the system size L is the dominant length scale and therefore substitutes for $\xi(T)$ in Eq. (5) to arrive at²⁰

$$JL^z/E = \chi_{\pm}(EL). \quad (7)$$

Strictly, this equation works only for $T = T_c$, but is also valid for $T \simeq T_c$ since leading order corrections are small: $O(L/\xi)$. In this powerful approach, there is only one fitting parameter, z , making its results more definitive.

To achieve the best scaling collapse for the FFH and FS scaling, the principle method that we use is to sort the data according to the value of the scaling variable x (whether it be $E\xi/T$ or EL) and then to minimize the difference of the logarithm of the values of two adjacent, scaled points using a least squares method.⁸ As a second means of optimization, we tried approximating the $T > T_c$ curve to a function and then minimizing the difference between the scaled points and the curve. However, because of the large number of fitting parameters, definitive results could not be achieved with this approach.

For various reasons, not all of the data are used in the optimization. At large values of the applied electric field ($E \simeq 0.8$), the isotherms become ohmic due to a saturation of the vortex density. (See discussion in Section IIIA.) Because this behavior is not due to critical behavior, the data should not scale (collapse) with the other data and so is not included in our optimization. However, we do plot those points in the scaling plots (Figures 2 and 6), even though those points do not collapse. (In Refs. 8,10 and 11, the analogous, large I data was not plotted with the scaled data.) In addition, because the dynamic critical exponent z has a temperature dependence below T_c due to the line of fixed points in the KTB critical behavior, the $T < T_c$ data are not used in the optimization of the FFH scaling collapse. This is because the temperature dependence of z is not the same as the scaling variable $x = E\xi/T$ and so the FFH scaling is not expected to be as effective in this regime.^{8,12} Nonetheless, we do scale the $T < T_c$ data assuming a symmetric correlation length. Finally, data are also excluded from the optimization if the error bars are greater than 50%.

III. RESULTS

The principal objectives of our work are to study the value of the dynamic critical exponent z for the 2DCG in the context of Fisher-Fisher-Huse scaling and the influence of finite size effects, and to study the behavior of the correlation length $\xi_-(T)$ below the phase transition.

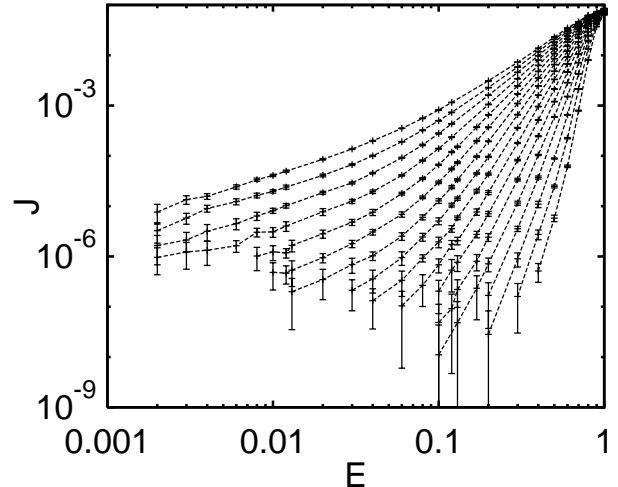


FIG. 1. Charge current density $J(E, T)$ versus E for fixed system size $L = 24$ for temperatures ranging from 0.09 to 0.25 by increments of 0.01 (from bottom to top).

A. Dynamic Critical Exponent z

The two principal system sizes used in our simulations were $L = 24$ and $L = 100$. The J - E isotherms for the $L = 24$ system are shown in Figure 1. As one can see the isothermal J - E curves mimic closely the V - I of thin-film superconductors.¹⁵ Reflecting the absence of vortex pairs, the higher temperature curves are primarily Ohmic (i.e., have slope 1 on a log-log plot). The lowest temperature curves are primarily non-Ohmic, indicating the presence of vortex pairs. The intermediate-temperature curves, on the other hand, are Ohmic for small E , become non-Ohmic at larger values of E , and abruptly turn Ohmic for the largest values of E . This of course reflects the fact that with each different value of E , one is probing a different length scale, which varies as the inverse of E .³² (See discussion in last paragraph of Section IIIB.) Consequently, at small E , long length scales are being probed where free vortices exist and Ohmic behavior is expected for $T > T_c$ (or when λ_\perp is finite). For large values of E , smaller length scales are probed where vortices are still bound in pairs and result in non-Ohmic behavior. The other salient feature of this graph is that the error bars become large at the small- E end of the isotherms due to small numbers of vortex pairs.

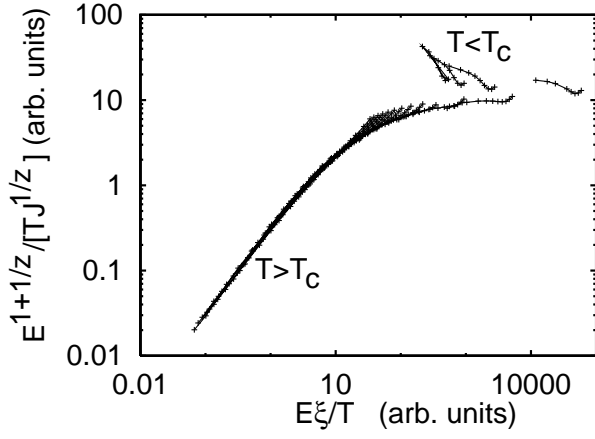


FIG. 2. The $L = 24$ data of Figure 1 scaled according to FFH scaling (Eq. 6) using $z = 6.01$, $T_c = 0.127$, and $C = 0.7475$.

The temperature of the phase transition in the $L = 24$ data is not obvious in Figure 1. Using the FFH dynamic scaling criteria for the critical isotherm, which says that $J \propto E^{z+1}$ for all values of E at $T = T_c$, results in $T_c \simeq 0.14$ and $z \simeq 6$. The subsequent FFH scaling for the $T > T_c$ data yields an excellent collapse for $z = 6.01$, $T_c = 0.127$, and $C = 0.7475$, as seen in Figure 2. (As noted in Section II, the crossover to Ohmic behavior at large E data seen Figure 1 is not due to critical behavior and so should not be used to judge the collapse. It is this large- E data that does not collapse with the other data in Figure 2.)

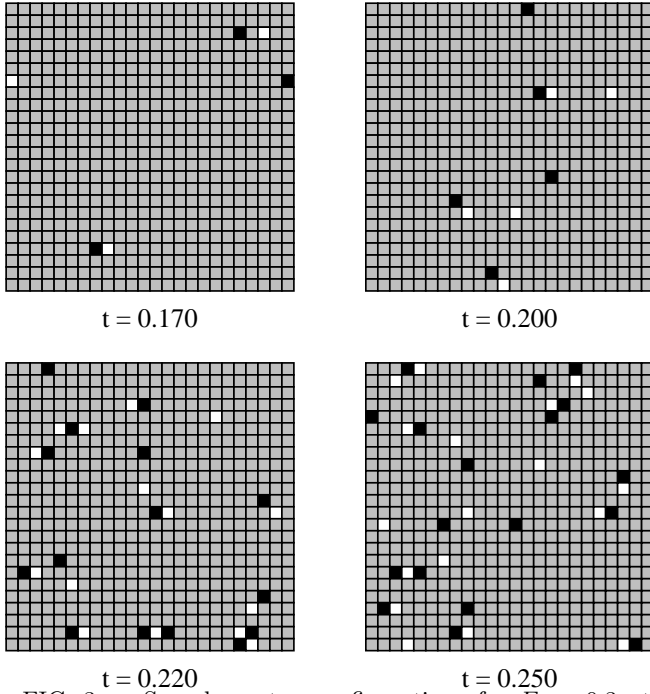


FIG. 3. Sample vortex configurations for $E = 0.3$ at four temperatures. A white box is a vortex, a black box an anti-vortex, and a grey box an empty lattice site.

The values of the parameters in this collapse, optimized using our method described in Section II, are consistent with the large values of z and low values of T_c found previously.^{8,10,11} However, an examination of the inverse dielectric constant²² ϵ^{-1} and the vortex density⁷ reveals no critical behavior at that temperature with or without a current. An inspection of the lattice configurations also reveals no clues of a phase transition at $T \simeq 0.13$. In Figure 3, characteristic vortex configurations in the lattice are shown for various temperatures for a relatively large value of the electric field, $E = 0.3$. Even at the lowest temperature shown here ($T = 0.17$), there are few vortices and they are clearly bound to one other. (One can also see in that figure that the vortices seem to become unbound above the expected T_c of 0.218.) Hence, the apparent FFH scaling collapse at the large value of z and the small value of T_c does not seem to correspond with a real phase transition. We now investigate if the FFH scaling collapse for these values of T_c and z could be due to finite size effects, as recently suggested by Medvedyeva *et al.*¹²

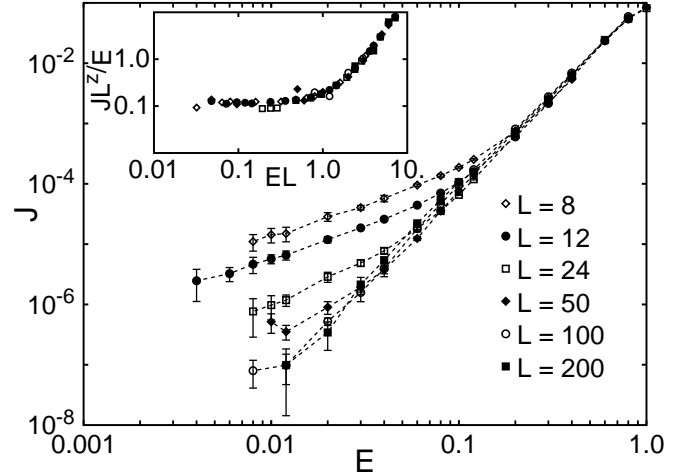


FIG. 4. The J - E curves for $T = 0.210$ for a variety of system sizes. [Inset: The same set of data scaled with finite size theory (Eq. 7) for $z = 2.15$.]

To further explore the value of z and the transition temperature, we employed finite-size scaling methods for $T = 0.210$, a temperature just below the expected value $T_c = 0.218$.^{22,33} The J - E curves for values of L ranging from 12 to 200 are shown in Figure 4. As one can see, the curves become straighter (on a log-log scale) as expected near the critical isotherm when the system size is increased, indicating that the low- E Ohmic behavior for the $L = 24$ data is attributable to finite size effects and that the true critical isotherm occurs at a larger temperature. The finite size scaling, shown in the inset to Figure 4, reinforces this idea. With z being the only fitting parameter, the optimal value is 2.15, reinforcing the original results of Lee and Teitel²⁰ (and the subsequent work of others) that $z = 2$ and that T_c occurs at a much larger value than obtained from the FFH scaling.

The fact that the value of z here is slightly larger than 2 can be attributed to the fact that the temperature is just below that of the expected value of the transition temperature and that z increases in value for $T < T_c$.

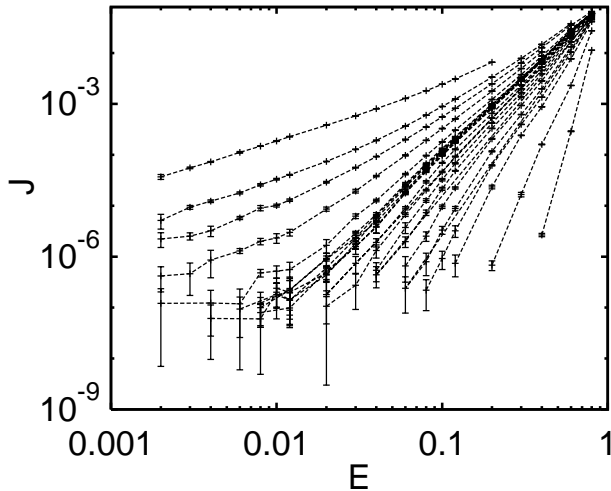


FIG. 5. Charge current density $J(E, T)$ versus E for fixed system size $L = 100$ for the temperatures 0.09, 0.12, 0.15, 0.16, 0.17, 0.18, 0.19, 0.195, 0.20, 0.205, 0.21, 0.211, 0.212, 0.213, 0.214, 0.215, 0.22, 0.23, 0.24, 0.25, 0.28 (from right to left). The density of curves is larger near T_c .

The value of z obtained in the finite size scaling reinforces the idea that the large value of z found for the $L = 24$ data in the FFH scaling is due to finite size effects. We have therefore calculated J - E curves for $L = 100$. (See Figure 5.) The J - E curves are similar to those of $L = 24$ both in terms of qualitative behavior and in terms of the error bars. The primary difference is that the intermediate-temperature curves are straighter than those of $L = 24$ and the critical isotherm now occurs at a temperature $T \simeq 0.210$ for $z \simeq 2$. (Of course, if we could extend the J - E data to smaller J , the J - E curves would not be straight for $T < T_c$ due to finite size effects.) Using these values as a guide, the best collapse for this data with the FFH scaling, shown in Figure 6, was obtained using $z = 1.90$, $T_c = 0.212$, and $C = 0.65$. As one can see, the collapse is quite good for the $T > T_c$ data. (Note that four points for $T = 0.22$ were excluded from this figure due to the fact that the error bars were greater than 50%.) Even the $T < T_c$ data scale well despite the fact that z in this regime has a temperature dependence different than that of the scaling parameter x . The $T = 0.090$ and $T = 0.12$ are the exception to the collapse but is most likely due to the fact that that data is well outside the critical region. The fact that the rest of the $T < T_c$ data scales reasonably well may be a coincidence or evidence for a finite correlation length. (We present evidence for a finite correlation length for $T < T_c$ in the next subsection.) The value of the T_c achieved through our methods is slightly smaller than the expected value,

which we attribute to finite size effects. We add that an acceptable collapse is also achieved for $T_c = 0.218$ and $z = 2$.

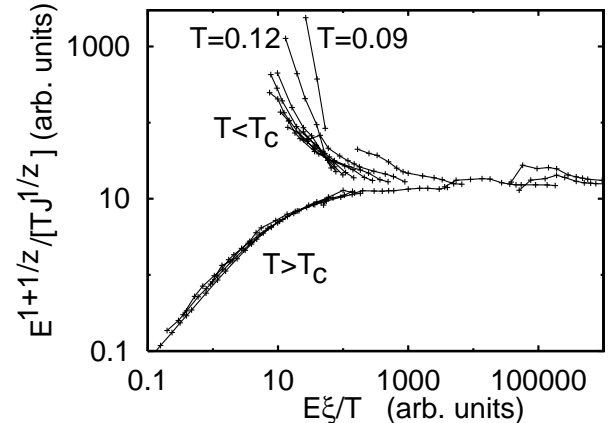


FIG. 6. The $L = 100$ data of Figure 5 scaled according to FFH scaling (Eq. 6) using $z = 1.90$, $T_c = 0.212$, and $C = 0.65$. The $T = 0.09$ and $T = 0.12$ isotherms do not collapse with the other curves, which we attribute to those curves being far from the critical region.

We believe that this work is a definitive verification of $z = 2.0 \pm 0.2$ found using FFH scaling and therefore puts FFH scaling in accord with finite size scaling. We conclude that the larger value of z (5.6) found for the $L = 24$ data and elsewhere^{8,10,11} is due to finite size effects.¹² (See discussion in Section IV.) This work also vindicates the use of FFH scaling for systems free of finite size effects. Lee and Teitel²⁰ and Harris *et al.*³⁴ have previously showed a $z = 2$ collapse using FFH scaling for their numerical data ($L = 24$) and JJA data, respectively. However, we do not believe that that work should not be taken as evidence for $z = 2$ because the scaling collapse was not convincing, they did not vary z to optimize the collapse, and it was later shown that the data collapse better for much larger values of z .^{8,11}

Finally, we note that we calculated the values of the J - E exponent α in order to study the predictions of Minnhagen *et al.*²⁵ about its temperature dependence. In accord with the work of others,^{23,24} our work indicates that the prediction of Ref. 25 for the temperature dependence of α (usually denoted α_{PM}) is in better agreement with the data than the original prediction³² for the temperature dependence of α (sometimes denoted α_{AHNS} .) This agreement further verifies our $L = 100$ J - E data.

B. Vortex Correlation Length for $T < T_c$

Our method for studying the vortex correlation length is to investigate the value of the J - E exponent α as a function of E by looking at the slope of our J - E curves. More specifically, we study the derivative $d \log J / d \log E$, which is equal to α when $J \propto E^\alpha$. A similar examination

by Medvedyeva *et al.*¹² (see their Figure 2) for system sizes of $L = 8$, using the analogous V - I curves in the 2D RSJ model, revealed that the slope started at a low value for small I , peaked, and then descended to a value near 1 at large values of I . For each of the isotherms with temperatures below the critical temperature, they found the peak to occur at roughly the same value of I .¹² Because the scaling variable is either $I\xi$ when $\xi \ll L$ or IL when $L \lesssim \xi$, the fact that the peak in $d \log V / d \log I$ does not move is an indication that finite size events dominate this temperature regime (and the scaling parameter is EL). Above T_c , the authors¹² found the peak to move quickly to larger values of I , indicating that $I\xi$ is the principal scaling variable since ξ is decreasing quickly in this regime.

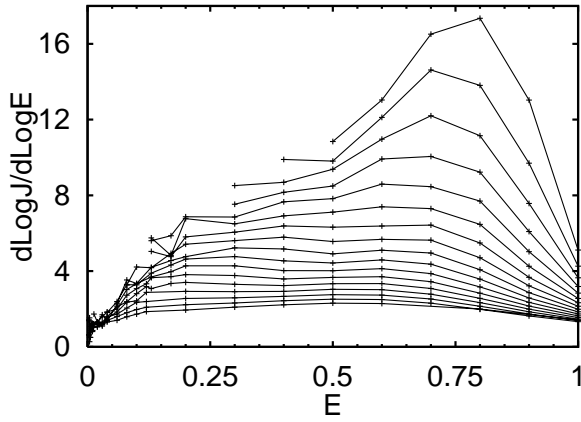


FIG. 7. The $L = 24$ J - E data plotted as $d \log J / d \log E$ versus E for all of the temperatures shown in Figure 1. The top curve corresponds to $T = 0.09$ and the bottom curve to $T = 0.25$.

For our $L = 24$ data, $d \log J / d \log E$ behaves differently below T_c than does the analogous quantity of Ref. 12. As one can see in Figure 7, the locations of the peaks as a function of E move to smaller values as one increases the temperature from 0.09 to about 0.14. In the temperature range 0.15-0.22, the peaks develop into plateaus.

The peaks and plateaus indicate that there are two competing length scales. On the large length scale side (small E) is the temperature-dependent correlation length $\xi_-(T)$ while at small length scales (large E) is the lattice size, which enters because of a saturation of vortex density. A plateau signifies that ξ is much larger than the saturation length scale while a peak indicates that ξ is approaching the lattice size. The value for the left hand size of the plateau is determined by ξ or L , whichever is smaller. In Figure 7, the point at which ξ becomes larger than L occurs at about $T = 0.19$, above which the plateau begins at $E \simeq 0.13$ on the low E side. That the value of E for which $d \log J / d \log E$ peaks or begins to plateau depends on temperature for a broad temperature range below T_c is an indication that the scaling variable for $T < 0.19 < T_c$ is $E\xi$ and that, therefore, $\xi_-(T)$ is

finite below T_c .

The lattice spacing affects the J - E curves for $E \gtrsim 0.7$, as can be seen in Figure 7, and determines a maximum value of E at which $d \log J / d \log E$ peaks. Therefore, the discrete lattice size can also result in the position of the peak in $d \log J / d \log E$ not moving. As a consequence, that the peaks would be located all at the same approximate value of E , as found in Ref. 12, should not be taken as evidence strictly for finite size effects.

The values of E that correspond to the influence of the lattice spacing and the lattice size can be predicted by simple arguments. (See for example Ref. 8.) The approximate energy for a vortex pair is $(\log R - ER)/\epsilon$, which increases for small R and then decreases for large R , thereby peaking at $R = 1/E$.²⁰ (This equation explains why one probes different length scales by changing the value of E as discussed in Section IIIA.) Since the lattice size corresponds to a value 1, one expects its effects to manifest themselves for $E \simeq 1$, which is what we observe in Figure 7. Similarly, one expects finite size effects to manifest themselves for $E \simeq 1/L \simeq 0.04$. Indeed, in Figure 7, all of the isotherms are ohmic for $E \lesssim 0.5$, in agreement with our prediction.

IV. DISCUSSION AND SUMMARY

Using system sizes up to $L = 200$ in Monte Carlo simulations of the 2DCG, we conclude $z = 2.0 \pm 0.2$ using Fisher-Fisher-Huse scaling and finite size scaling, reinforcing the results of others that $z = 2$. (See, e.g., Refs. 12,20,21.) We have also presented evidence that ξ_- , the correlation length below T_c , is finite.

Previous analysis of experimental data on 2D superconductors, JJA's, and superfluids, and of numerical data on the 2DCG by two of these authors^{8,10,11} using FFH scaling indicated $z \simeq 5.6$. As stated here and in Ref. 12, it appears that this large value is due to finite size effects. Because a majority of the V - I data from the literature was examined in Ref. 8, it appears that nearly all experimental V - I measurements on 2D superconductors and JJA's are dominated by finite size effects. Why the value $z \sim 6$ should result from finite size effects¹² remains a mystery, and should be studied further.

Because these results indicate that finite size effects are ubiquitous in 2D superconductors and 2D JJA's, the V - I and R data from the literature that were used to verify KTB behavior in the conventional manner needs to be re-examined to account for the finite size effects. In the presence of strong finite size effects like those in these samples, two aspects of the conventional method fail. First, the small I behavior of the V - I isotherms would not reveal any quick changes in α near T_c because finite size effects dominate at small I . In other words, as is well known, finite size effects wash out the expected jump in α . Secondly and more importantly, the resistance formulas are no longer valid in the presence of fi-

nite size effects. That previous authors could fit their resistance data to the more commonly used Minnhagen formula is most likely due to the number of fitting parameters. Finally, we stress that the most effective means for studying the temperature dependence of α should begin by extracting $\alpha(T)$ from the V - I curves in 2D superconductors and JJA's for the same value of I .

Clearly, in order for this data to be re-interpreted, a better understanding of finite size effects is needed since previous checks for finite size effects in the data of Ref. 15 were negative. For example, those authors¹⁵ found that the value of $\lambda_{\perp}(0)$ derived from a fit to $\lambda_{\perp}(T)$ was four times larger than the expected value. Furthermore, for that same data,¹⁵ where finite size effects are now known to dominate, the resistance was found to fit better to the Kosterlitz resistance formula than a resistance formula derived for finite-size dominated Ohmic resistance.⁸ Finally, in Ref. 8, it was found that the length scale at which the crossover from finite-size-induced Ohmic behavior to non-Ohmic behavior was expected to occur for the data of Ref. 15 did not correspond with the observed value.

ACKNOWLEDGMENTS

Acknowledgement is made by SWP to the donors of The Petroleum Research Fund, administered by the ACS, for support of this research.

* Electronic address: lcolonna@wpi.edu.

† Electronic address: pierson@wpi.edu.

‡ Electronic address: friesen@cae.wisc.edu.

¹ J. M. Kosterlitz and D. J. Thouless, J. Phys. C **6**, 1181 (1973).

² J. M. Kosterlitz, J. Phys. C **7**, 1046 (1974).

³ V. L. Berezinskii, Sov. Phys. JETP **32**, 493 (1971).

⁴ J. C. Garland and H. J. Lee, Phys. Rev. B **36**, 3638 (1987).

⁵ A. T. Fiory, A. F. Hebard, and W. I. Glaberson, Phys. Rev. B **28**, 5075 (1983).

⁶ T. K. Shaw, M. J. Ferrari, L. L. Sohn, D.-H. Lee, M. Tinkham, and J. Clarke, Phys. Rev. Lett. **76**, 2551 (1996); C. Timm, Phys. Rev. B **55**, 3241 (1997).

⁷ For a review, see P. Minnhagen, Rev. Mod. Phys. **59**, 1001 (1987); and references therein.

⁸ S. W. Pierson, M. Friesen, S. M. Ammirata, J. C. Hunnicutt, and L. A. Gorham, Phys. Rev. B **60**, 1309 (1999).

⁹ D. S. Fisher, M. P. A. Fisher, and D. A. Huse, Phys. Rev. B **43**, 130 (1991).

¹⁰ S. M. Ammirata, M. Friesen, S. W. Pierson, L. A. Gorham, J. C. Hunnicutt, M. L. Trawick, and C. D. Keener, Physica C **313**, 225 (1999).

¹¹ S. W. Pierson and M. Friesen, Physica B **284-288**, 610 (2000).

¹² K. Medvedyeva, B. M. Kim, and P. M. Minnhagen, Phys. Rev. B (in print).

¹³ J. Pearl, Appl. Phys. Lett. **5**, 65 (1964).

¹⁴ A. M. Kadin, K. Epstein, and A. M. Goldman, Phys. Rev. B **27**, 6991 (1983).

¹⁵ J. M. Repaci, C. Kwon, Q. Li, X. Jiang, T. Venkatesan, R. E. Glover, C. J. Lobb, and R. S. Newrock, Phys. Rev. B **54**, R9674 (1996).

¹⁶ S. T. Herbert, Y. Jun, R. S. Newrock, C. J. Lobb, K. Ravindran, H.-K. Shin, D. B. Mast, and S. Elhamri, Phys. Rev. B **57**, 1154 (1998).

¹⁷ M. V. Simkin and J. M. Kosterlitz, Phys. Rev. B **55**, 11646 (1997).

¹⁸ A. N. Artemov, JETP Letters **68**, 492 (1998).

¹⁹ S. W. Pierson and O. T. Valls, Phys. Rev. B **61**, 663 (2000).

²⁰ J.-R. Lee and S. Teitel, Phys. Rev. B **50**, 3149 (1994).

²¹ P. H. E. Tiesinga, T. J. Hagenaars, J. E. van Himbergen and J. V. José, Phys. Rev. Lett. **78**, 519 (1997).

²² J.-R. Lee and S. Teitel, Phys. Rev. B **46**, 3247 (1992).

²³ K. Holmlund and P. Minnhagen, Phys. Rev. B **54**, 523 (1996).

²⁴ H. Weber, M. Wallin, and H. J. Jensen, Phys. Rev. B **53**, 8566 (1996).

²⁵ See, e.g., A. Jonsson and P. Minnhagen, Phys. Rev. Lett. **55**, 9035 (1997); and references therein.

²⁶ B. J. Kim, P. Minnhagen, and P. Olsson, Phys. Rev. B **59**, 11506 (1999).

²⁷ M. Friesen, Phys. Rev. B **51**, 632 (1995).

²⁸ S. W. Pierson, Phys. Rev. B **51**, 6663 (1995).

²⁹ See, e.g., B.I. Halperin, *Physics of Low-Dimensional Systems*, Proceedings of the Kyoto Summer Institute, edited by Y. Nagaoka and S. Hikami, (Kyoto: Publication Office, *Progress in Theoretical Physics*, 1979) p. 53; S. Pierson, Phil. Mag. B **76**, 715 (1997); or R. J. Creswick, H. A. Farach, and C. P. Poole, *Introduction to Renormalization Group Methods in Physics*, (John Wiley & Sons, Inc., New York, 1992).

³⁰ N. Metropolis, A. W. Rosenbluth, M. N. Rosenbluth, A. H. Teller, E. Teller, J. Chem. Phys. **21**, 1087 (1953).

³¹ See, e.g., M. P. Allen and D. J. Tildesley, *Computer Simulations of Liquids* (Clarendon Press, Oxford, 1991).

³² V. Ambegaokar, B. I. Halperin, D. R. Nelson and E. D. Siggia, Phys. Rev. B **21**, 1806 (1980).

³³ M. Wallin and H. Weber, Phys. Rev. B **51**, 6163 (1995).

³⁴ D. C. Harris, S. T. Herbert, D. Stroud, and J. C. Garland, Phys. Rev. Lett. **67**, 3606 (1991).